Journal of Microwaves, Optoelectronics and Electromagnetic Applications, Vol. 20, No. 4, December 2021
DOI: http://dx.doi.org/10.1590/2179-10742021v20i4254763

Methodology for Minimizing Electric Field at Ground Level from Transmission Lines Using Sensitivity Analysis

A. L. Paganotti [1], R. R. Saldanha [1], A. C. Lisboa [1], M. M. Afonso [2], M. Q. Melo [2], M. A. O. Schroeder [2]
[1]*Graduate Program in Electrical Engineering, Universidade Federal de Minas Gerais, Belo Horizonte, Brazil*
paganotti@cefetmg.br, rodney@cpdee.ufmg.br, adrianochaves@cefetmg.br
[2]*Electrical Engineering Postgraduate Program, UFSJ-CEFET-MG, Belo Horizonte, Brazil*
marciomatias@cefetmg.br, marcilioq@yahoo.com.br, schroeder@ufsj.edu.br

***Abstract*– In this paper, a new methodology is applied to optimize the geometry of conductors of overhead transmission lines (TL) with high precision and low computational cost. This methodology is based on the sensitivity analysis of the electrical charge of the transmission lines using the adjoint method. This information is used with the gradient method and the golden section algorithm to minimize the electric field at the ground level of three-phase TL with two cables per phase. The approximation using central finite differences to obtain sensitivity is adopted for validation and comparisons. The TL's with high surge impedance loading is obtained after the optimization process.**

***Index Terms*–** Adjoint Method, Electric Charge, Gradient Method, Sensitivity Analysis, Transmission Lines.

I. Introduction

The Brazilian country has continentality dimensions and needs to transmission energy from generator centers to consumer centers in different regions of the country. It generates the necessity of to built very long transmission lines with high investment involved [1]. New methodologies has been developed on the last decades for to get TL with higher capacity of transmission energy than conventional ones [2]–[4].

The increase in the power transmission capacity can be achieved by conventional uprating techniques applied on transmission lines, such as: increasing the thermal limit of the line [5], [6]; increasing operating voltage; increasing the number of subconductors per phase [7], [8]; or using compensators [8], among other methodologies.

The Russian researchers has been developed since 70's an unconventional and highly viable alternative called high surge impedance loading (HSIL) lines [9]–[11]. This methodology have commissioned TL's in operation on Russian and Brazilian territories [4], [12].

The HSIL implementation involves rearranging or increasing the number of conductors per bundle to equalize the electric field between them. The HSIL methodology is based on the understanding of the behavior of the electric field associated with each cable and how the physical and geometric parameters of the line affect the electric field distribution [13], [9], [11]. The first geometric optimization of the bundles study was presented in [14], where the main objective was to reduce audible noises.

The optimization of transmission lines to improve the SIL using conventional circular, circular augmented, and elliptical bundles for equalization of electric field and current between the subcondutors

Brazilian Microwave and Optoelectronics Society-SBMO *received 29 Jan 2021; for review 29 Jan 2021; accepted 29 Apr 2021*
Brazilian Society of Electromagnetism-SBMag *ISSN 2179-1074*

is presented in [15]. The optimization of conductor bundles with single and multiple circuits using evolutionary methods is performed in [3], [16], using approximated models for TL. The gradient project method has been used in the design of new transmission lines with non-conventional shapes in [17]. In [18] a new methodology takes the optimization of HSIL lines without change the bundle shapes, only change the centroids of each bundle. The ellipsoidal method, proposed in [19] is adopted by [18] for minimizing electric field at ground level. A complete description of the technological challenges involved in implementing HSIL methodology is given by [11].

Here the sensitivity analysis of the electric field at the ground level using the adjoint method is developed [20]. This method has been used successfully in weather forecasting studies, in high frequency electromagnetic problems and in problems with a high number of variables [21]–[23].

The adjoint method gets the sensitivity analysis (derived from the objective function concerning the parameter of interest) of a problem solving only one more linear system of equations. While using a classical method like the finite differences method, it is necessary to solve a system of equations for each variable involved [21]. The adjoint method is efficient and fast to obtain the gradient information of the objective function. The gradient, ellipsoidal and quasi-Newton methods are examples of search direction methods that work with the sensitivity information obtained by the adjoint method [24], [2].

The adjoint method applied in low-frequency electromagnetic problems related to bundle optimization is not available in the literature and it represents the main contribution of this paper. The assessment of sensitivity by the adjoint method is based on Telegen's principle and has been applied to high-frequency optimization problems auspiciously [25].

In this paper, a tool to calculate and minimize the electric field at the ground level and improve the SIL of the TL is developed. An electromagnetic model of the TL understudy is developed and the electric charge and the electric field strength of the system are obtained. The optimization process is performed by the gradient method which uses the sensitivity obtained by the adjoint method and the approximation given by the central finite differences (CFD).

This paper enrolls as follows. Section II presents TL modeling. In Section III the adjoint modeling is presented. Section IV presents an introduction to the optimization method adopted. In Section V the surge impedance loading of TL is discussed. In section VI, the results of the simulations are presented. The conclusions are presented in Section VII.

II. Transmission Line Modeling

The TL analyzed is under normal steady-state operating conditions. The domain where the TL is inserted, is considered to be linear, homogeneous, and isotropic [5], [26]. For the electric field evaluation, the TL conductors are modeled as being straight, cylindrical, of infinite length, without losses, and parallel to the ground plane. The soil effect is taken into account using the image method. The electrical charge for each conductor is obtained using Maxwell's potential coefficient matrix [26], [5]:

$$\begin{bmatrix} q_a \\ q_b \\ q_c \end{bmatrix} = \begin{bmatrix} P_{aa} & P_{ab} & P_{ac} \\ P_{ba} & P_{bb} & P_{bc} \\ P_{ca} & P_{cb} & P_{cc} \end{bmatrix}^{-1} \begin{bmatrix} V_{an} \\ V_{bn} \\ V_{cn} \end{bmatrix} \tag{1}$$

where q_a, q_b and q_c are the electric charge phasors of each phase, V_{an}, V_{bn} and V_{cn} are the voltage phasors applied in each phase. The description of the elements of Maxwell's potential coefficient

ISSN 2179-1074

matrix can be obtained from [5], [26]. Once the electrical charge for each cable is defined, the x and y components of the electric field at ground level can be obtained by applying Gauss's law. The electric field in the x direction E_x is given by [5], [26]:

$$E_x(x,y) = \sum_{i=1}^{N} \left(\frac{q_i}{2\pi\epsilon_0}\right) \left[\frac{(x_n - x_i)}{(x_n - x_i)^2 + (y_n - y_i)^2} - \frac{(x_n - x_i)}{(x_n - x_i)^2 + (y_n + y_i)^2}\right]^2 \tag{2}$$

where q_i is the electrical charge of the $i-th$ conductor, x_i and y_i, x_n and y_n, respectively horizontal and vertical positions of conductors and field assessment points; and N is the number of conductors. The intensity of the electric field depends on the position and electrical charge of each conductor. Besides, capacitance and inductance of the TL, are defined by conductor geometries, these parameters are directly related to the transmission capacity of the TL [27].

Along the surface of each cable of the TL, the superficial electric field is determined. The successive image method is adopted, described in detail by [28]. The maximum surface electric field of each cable is compared with the value of the critical surface electric field (E_c) from which the corona effect occurs [29], [11]:

$$E_c = 18.11 f_s \delta_{ik} \left(1 + \frac{0.54187}{\sqrt{r\delta_{ik}}}\right) \tag{3}$$

where r is the radius of the conductor in cm, f_s is the surface factor, usually adopted as 0.82, and δ_{ik} is the atmospheric pressure at sea level [10]. A sensitivity analysis of the electrical charge of the transmission system related to cable position (coordinates x and y) can be obtained precisely and fast, using the adjoint method presented in the next section.

III. Sensitivity Analysis

The electrical charge of each conductor of the TL is obtained through the linear system of equations given by:

$$P(x,y)q = V \tag{4}$$

where $P(x,y)$ is the $(N \times N)$-matrix of the system (the elements of this matrix are dependent on the design variables x and y), N is the number of TL conductors, q is the N-vector of state variables and V is the excitation N-vector.

The objective of the adjoint sensitivity is to obtain the gradient of a response function (objective) of interest defined by the user $f(x,y,q)$ regarding the coordinates x and y of the problem. The classic way to achieve this gradient is through the finite difference method. It perturb each parameter related to x_i and y_i and solves the linear systems obtained from it. This approach needs to obtain $P(x,y)$ for each disturbed parameter and solve the linear system at least n times, where n is the number of disturbing variables [21].

The adjoint method can determine the derivate of the objective function (sensitivity) more efficiently. The sensitivity analysis concerning the x coordinate is given as follows. It starts with the differentiation of the linear system given in (4) in relation to the i-th parameter x_i [20]:

$$\frac{\partial(P(x)\bar{q})}{\partial x_i} + P\frac{\partial q}{\partial x_i} = \frac{\partial V}{\partial x_i} \tag{5}$$

The first term of (5) consists of the derivative of the matrix P while q is maintained at its nominal value $\bar{q}$. The expression (5) is rewritten according to the state variable q:

$$\frac{\partial q}{\partial x_i} = P^{-1}\left(\frac{\partial V}{\partial x_i} - \frac{\partial (P\bar{q})}{\partial x_i}\right) \tag{6}$$

The derivative of the objective function $f(x, q)$ in relation to the i-th parameter x_i is given by [20]:

$$\frac{\partial f}{\partial x_i} = \frac{\partial^e f}{\partial x_i} + \left(\frac{\partial f}{\partial q}\right)^T P^{-1}\left(\frac{\partial V}{\partial x_i} - \frac{\partial (P\bar{q})}{\partial x_i}\right) \tag{7}$$

The adjoint variable is inserted in (7), which is responsible for the connect the design variables of the problem (x, y) and the objective function [20], [30]:

$$\hat{q}^T = \left(\frac{\partial f}{\partial q}\right)^T P^{-1} \tag{8}$$

$$\Rightarrow P^T\hat{q} = \left(\frac{\partial f}{\partial q}\right) \tag{9}$$

The $\hat{q}$ vector of adjoint variables is obtained by solving (9). The adjoint matrix of the system is the transposition of the original system given by (4). The excitation of the adjoint system (9) depends on the objective function $f(x, q)$ and it's derivative in relation to the state variables. Solving the adjoint system the sensitivity of the response of the i-th parameter x_i is given by [20]:

$$\frac{\partial f}{\partial x_i} = \frac{\partial^e f}{\partial x_i} + \hat{q}^T\left(\frac{\partial V}{\partial x_i} - \frac{\partial (P\bar{q})}{\partial x_i}\right) \tag{10}$$

It's verified that with the solution of the original system (4), q is obtained while solving the adjoint system (9) $\hat{q}$ is derived. Then the sensitivity related to each parameter x can be obtained by means of (10). The objective function $f(x, q)$ related to the proposed problem is given by:

$$f(x, q) = \left(\sum_{i=1}^{N} q_i\right)^2 \tag{11}$$

where N is the number of TL conductors and q_i is the density of charge of each conductor. The derivative of the response function adopted as an excitation vector in the adjoint model is given by:

$$\frac{\partial f(x, q)}{\partial q} = 2\left(\sum_{i=1}^{N} q_i\right) \tag{12}$$

The response function adopted $f(x, q)$ and the voltage phasor V used to calculate the electrical charge of the system have no dependence on x variable, leading these terms to vanish in (10). So, the expression of the sensitivity analysis obtained with the adjoint method concerning x_i is finally obtained:

$$\frac{\partial f(x, q)}{\partial x_i} = \hat{q}^T\left(-\frac{\partial P}{\partial x_i}\right)\bar{q} \tag{13}$$

where $\hat{q}$ is obtained solving the adjoint system, and q is obtained from the original system solution. With the adjoint modeling of the problem, it is possible to get information on the sensitivity of n variables just by solving one more linear system.

The adjoint method needs to evaluate the derivative of the matrix of the system $P(x, y)$. If the derivate

Brazilian Microwave and Optoelectronics Society-SBMO received 29 Jan 2021; for review 29 Jan 2021; accepted 29 Apr 2021
Brazilian Society of Electromagnetism-SBMag

ISSN 2179-1074

of $P(x,y)$ matrix is given numerically by using the central finite difference (CFD) approximation, the adjoint-CFD method of sensitivity analysis is obtained [21]. This sensitivity is called feasible adjoint sensitivity technique (FAST) proposed by [31]. However, if the analytic derivate of the $P(x,y)$ matrix is performed, so the sensitivity analysis is called adjoint-analytic method [31]. Once the methodology for obtaining the gradient information is defined, the next step is to choose an optimization method that uses it.

IV. Optimization Method

The optimization method adopted uses the gradient of the objective function obtained through the adjoint and CFD methods described in detail in the previous section. The gradient method with the golden section algorithm is adopted in this work. The method is defined by the iterative algorithm, [21]:

$$x_{k+1} = x_k - \alpha_k \nabla f(x_k) \tag{14}$$

where the new minimum x_{k+1} is obtained by a step of length α_k towards the opposite direction of the gradient of the objective function. The step length α_k is a scalar minimizing the objective function towards $-\nabla f(x_k)$ which is obtained via the algorithm of the gold section [21].

In (14) from the point x_k a new minimum point is obtained along the opposite direction of the gradient of the objective function, this minimum is adopted as x_{k+1}. α is a scalar minimizing term that changes with each iteration and is obtained via the algorithm of the gold section [21]. The only necessary condition for the application of this algorithm is that the function is differentiable. The complete description of this algorithm is given by [24]. The objective function of this work is given by the square of the sum of the electric charge intensities of each TL conductor obtained by (1) and represented by (11).

During the optimization process, the cable height can range from 1.00 m above ($H\max$) or below ($H\min$) the original vertical positions. The restrictions adopted during the optimization process are shown in Fig. 1.

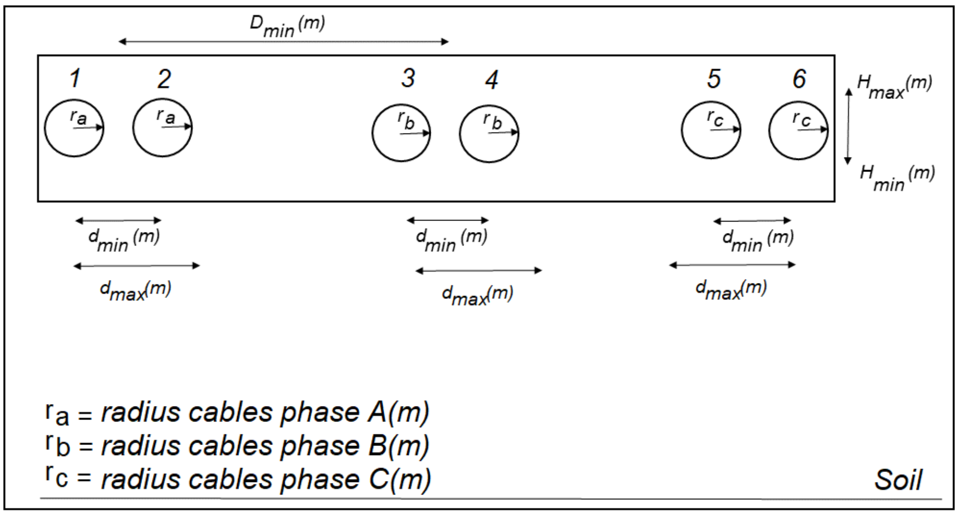

Fig. 1. Geometric constraints adopted during optimization process: D_{min} is the minimum distance between conductors of different phases; d_{min},d_{max} are the respective: minimum and maximum distance between conductors of the same bundle; H_{min}, H_{max} are the respective: minimum and the maximum height of each cable.

In Fig. 1 $D\mathrm{min}$ determines the minimum distance between different phases and $d\mathrm{min}$ determines the minimum distance between conductors of the same phase. Another constraint adopted during the optimization process is the maximum distance between conductors of the same bundle $d\mathrm{max}$. This constraint is used to avoid solutions with bundles with large dimensions. This constraint search for feasible solutions related to mechanical implementation aspects [11], [3].

The other constraint adopted in the optimization process is related to Brazilian law. The federal legislation [32] and the NBR 25415 [33], [34], establish the reference levels of electric fields at ground level for occupational and general public exposure as 8.33 kV/m and 4.16 kV/m, respectively. Here, 1 m above the soil these levels of electric fields are verified through all the right-of-way (ROW) extension of the transmission lines.

The maximum electric field at the surface of each conductor must the lower than or equal to the critic electric field at the surface of the conductor obtained by (3). This constraint is to avoid the corona effect occurrence in the optimized geometries.

During the optimization process, the number of variables in the optimization problem is half of the real problem. This is because horizontally symmetric geometries are desired. This strategy saves computational time during the optimization process and searches for solutions with equal mechanical efforts in the tower arms.

To simplify the optimization process, shield wires are disregarded: their effect on the electric field profile at ground level is negligible [28]. The mechanical and structural feasibility of the suggested configuration by optimization must be analyzed through technical studies of mechanical efforts, costs, among others [35].

The last constraint established that the SIL of the new geometry suggested must be bigger than or the same as the original one after the optimization process developed in this work. The surge impedance loading (SIL) is discussed in the next section.

V. Surge Impedance Loading

The surge impedance loading (SIL) of TL's is given in MW and is obtained when the reactive balance occurs [1]. The characteristic impedance Z_c is expressed as the reactive power produced is equal to the reactive power consumed. This relationship is expressed by [1]:

$$Z_c = \frac{V_{ff}}{I} = \sqrt{\left(\frac{L}{C}\right)} \tag{15}$$

where V_{ff} is the magnitude of the phasor voltage between two phases [kV], I is the line current [A], L is the line inductance of the positive sequence per meter [H / m], C is the line capacitance of the positive sequence per meter [C/m] and Z_c is the characteristic impedance [Ω]. The SIL can be expressed as [1]:

$$SIL = \frac{{V_{ff}}^2}{Z_c} \tag{16}$$

From (16) and (15), an increase in the surge impedance loading can be obtained by increasing C and/or reducing L of the TL. High surge impedance loading lines (HSIL) have been used to reduce the right-of-way width of the TL's (distances between different phases reduced) and using bundles with increasing distance between subconductors. These actions intend to reduce Z_c and improve the SIL [13].

Brazilian Microwave and Optoelectronics Society-SBMO received 29 Jan 2021; for review 29 Jan 2021; accepted 29 Apr 2021

ISSN 2179-1074

VI. Results

Here a 345 kV TL with 2 cables per phase, is considered to show the effectiveness of the proposed approach. The adopted geometric constraints are shown in Table I, where X_L and X_R are the left and right horizontal limits and the other parameters are shown in Fig.1. The last constraint is concerned with the SIL. It requires that the SIL of the new geometries must be greater than 5% of the original ones.

Table I. CONSTRAINTS OF OPTIMIZATION PROCESS

Case	$\mathbf{D}_{\min}$(m)	$\mathbf{d}_{\min}$(m)	$\mathbf{d}_{\max}$(m)	$\mathbf{X_L}$(m)	$\mathbf{X_R}$(m)	$\mathbf{H}_{\max}$(m)	$\mathbf{H}_{\min}$(m)
I	5.00	0.40	1.50	-9.46	9.46	15.29	13.29

The gradient of the objective function is obtained in three different ways: first, with the adjoint-CFD method, second using the adjoint-analytic method, and third, using the CFD method. The errors 1 and 2 obtained between CFD and adjoint-CFD methods and between CFD and adjoint-analytic methods, respectively, for the sensitivity analysis, is shown in Table II.

Table II. COMPARATIVE ERROR - ADJOINT AND CFD METHODS

Case I - cable 1	Sensitivity in x	Sensitivity in y
Adjoint-CFD method	$0.1021497399422\times10^{-11}$	$0.3558566740333\times10^{-13}$
Adjoint-analytic method	$0.1021497406179\times10^{-11}$	$0.3558566672820\times10^{-13}$
CFD method	$0.1021497399190\times10^{-11}$	$0.3558565644821\times10^{-13}$
|Error 1|	$2.2711749261239\times10^{-10}$	$3.0785212630365\times10^{-7}$
|Error 2|	$6.8419164419323\times10^{-9}$	$2.8888015643788\times10^{-7}$

Table II show the errors of the sensitivity analysis obtained by the adjoint-CFD, adjoint-analytic, and CFD methods for the conductor number 1 of the TL shown in Fig. 1. It's verified that the sensitivity in x and y obtained through the adjoint method has high precision with errors from the sixth decimal place.

The algorithm takes 100 iterations to find the optimal solution. The profile of the original and optimized electric field using the gradient method that uses the sensitivity obtained by the adjoint-CFD, adjoint-analytic, and CFD methods can be seen in Fig. 2. Fig. 2 shows that the application of the gradient method that uses the sensitivity information obtained through the adjoint method obtains a configuration with reduction of the electric field at ground level. The original and optimized positions of the cables can be seen in Fig. 3. Fig. 3 shows that the bundles obtained are symmetrical and have lower distances between phases. The final configuration is given by gradient method using adjoint-CFD, adjoint-analytic, and CFD sensitivity are different. The starting and ending positions of the cables are given in the Table III.

Brazilian Microwave and Optoelectronics Society-SBMO received 29 Jan 2021; for review 29 Jan 2021; accepted 29 Apr 2021
Brazilian Society of Electromagnetism-SBMag ISSN 2179-1074

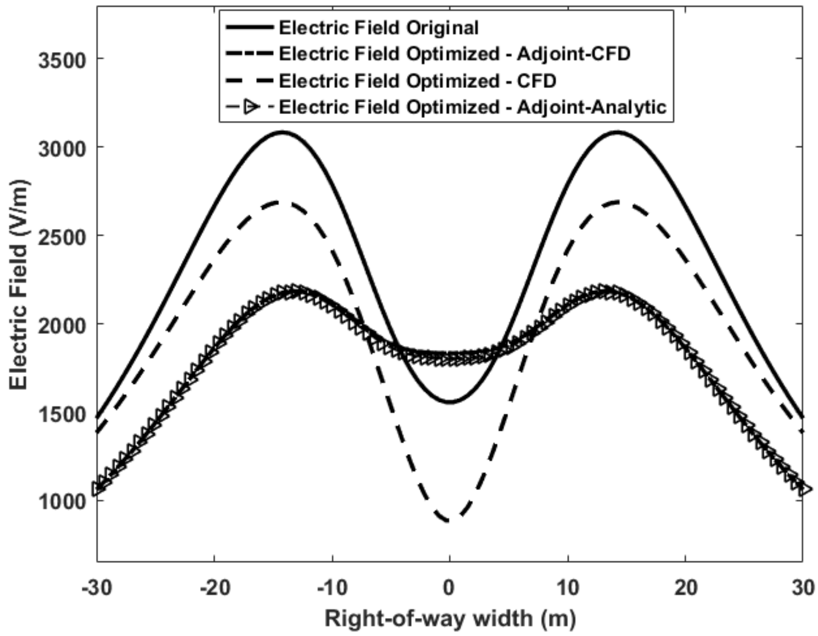

Fig. 2. Electric field profile at the ground level - original and optimized.

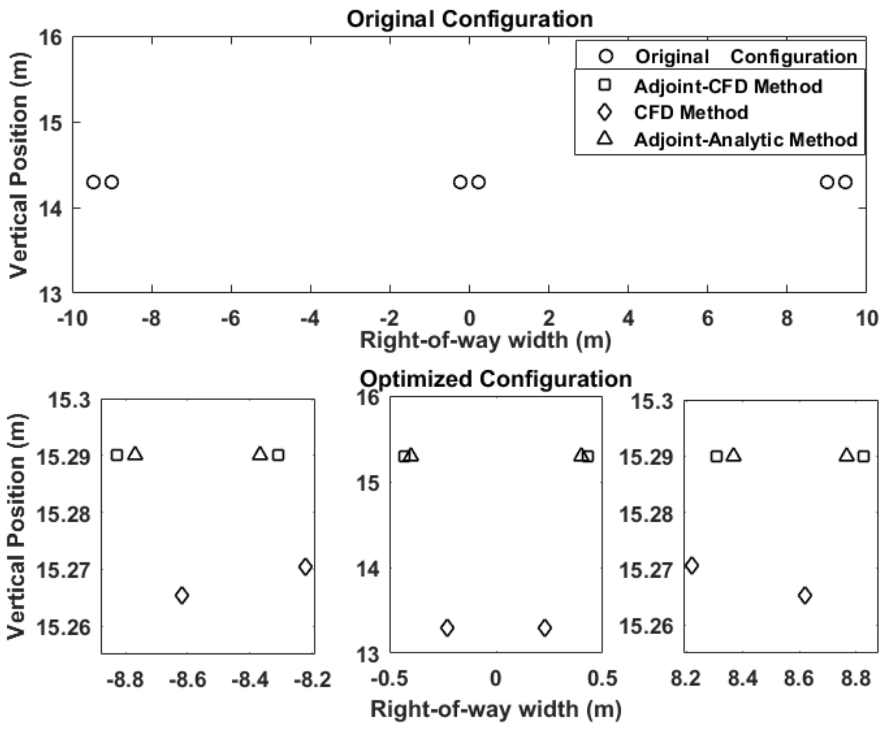

Fig. 3. TL 02 cables $345kV$ - original configuration (○),
optimized configuration: adjoint-CFD method (□), adjoint-analytic method (△), CFD method (⋄).

TABLE III. ORIGINAL AND OPTIMIZED POSITIONS

Positions	Phase 1 (m)	Phase 2 (m)	Phase 3 (m)
x original	-9.457 -9.000	-0.228 0.228	9.000 9.457
x optimized adjoint-CFD	-8.826 -8.307	-0.431 0.431	8.307 8.826
x optimized CFD	-8.620 -8.220	-0.228 0.228	8.220 8.620
x optimized adjoint-analytic	-8.769 -8.369	-0.399 0.399	8.369 8.769
y original	14.290 14.290	14.290 14.290	14.290 14.290
y optimized adjoint-CFD	15.290 15.290	15.290 15.290	15.290 15.290
y optimized CFD	15.265 15.270	13.290 13.290	15.270 15.265
y optimized adjoint-analytic	15.290 15.290	15.290 15.290	15.290 15.290

The maximum value for the electric field at surface of each conductor is obtained for: the original configuration (E_s original); the configuration obtained using adjoint-CFD method (E_s adjoint-CFD); the configuration obtained using adjoint-analytic method (E_s adjoint-analytic); the configuration obtained using CFD method (E_s CFD). These maximum values are compared with the critical value of the electric field at the surface (E_s critical) of the cables. All of these superficial electric field levels are presented in Table IV. It shows that the optimization configurations have a satisfactory behavior concerning the occurrence of the corona effect because the critical value of the superficial electric field in each cable is respected.

TABLE IV. MAXIMUM AND CRITICAL SUPERFICIAL ELECTRIC FIELD INTENSITIES

Cable number	E_s original (kV/cm)	E_s adjoint-CFD (kV/cm)	E_s adjoint-analytic (kV/cm)	E_s CFD (kV/cm)	E_s critical (kV/cm)
1	16.136	17.934	17.544	17.790	19.377
2	17.601	18.889	18.676	18.286	19.377
3	16.548	17.080	16.824	16.968	19.377
4	16.552	17.079	16.824	16.968	19.377
5	17.604	18.891	18.678	18.287	19.377
6	16.138	17.932	17.542	17.789	19.377

The surge impedance loading (SIL), the characteristic impedance (Z_c) of the original, and optimized configurations, and the computational time of different methods of sensitivity are given in Table V.

TABLE V. SURGE IMPEDANCE LOADING (SIL) AND CHARACTERISTIC IMPEDANCE (Z_c)

Case I	Original	CFD method	Adjoint-CFD method	Adjoint-analytic method
Z_c (Ω)	294.40	248.33	265.30	271.05
SIL (MW)	404.29	479.30	448.63	439.12
Increase in SIL (%)		18.55	10.97	8.61
Computational Time		t	t/3.80	t/6.32

It could be observed from Table V that the impedance Z_c, in the optimized configurations, are lower than the original one. The relation between SIL and Z_c is given by (16) where it is possible to see that the SIL grows when Zc decreases.

Although the proposed optimization problem is based on the minimization of electric charge of the conductors (11), the improvements in the SIL are, respectively, 18.55%, 10.97%, and 8.61% using CFD, adjoint-CFD, and adjoint-analytic methods. Also, once the SIL is a constraint in the problem, it is expected that for more complex cases (a great number of conductors) the constraints would be more difficult to be respected due to the increase in the number of variables which requires more time of execution for CFD method. On the other hand, the sensitivity analysis using the adjoint methods is not affected by the choice of perturbation parameters and does not demand additional computational time with a large number of variables. So, the bigger value of the SIL found by the CFD method in this specific case does not guarantee that it would happen for other cases with more than two cables per phase.

Finally, it is important to highlight the reduction of the computational time using the adjoint method compared with CFD methods in Table V. The time to calculate the sensitivity using adjoint-CFD and adjoint-analytic methods are 3.8 and 6.32 times lower than the computational time of the CFD method. This is because, with only the solution of one more linear system, the adjoint sensitivity concerning the n variables considered is obtained. On the other hand, in the CFD approach, it is necessary to have the solution of a system with forwarding and backward perturbation for each one of the n evaluate variables.

VII. Conclusions

The proposed methodology furnished configurations with improved SIL and reduced electric fields at ground level. It's verified that the sensitivity analysis using the adjoint method provides the gradient information with higher precision and greater efficiency than the approximation using central finite differences.

The results shows that the sensitivity analysis has the potential to be used in cases with a greater number of conductors per phase. Also, this method can become the optimization process more faster by reducing the computational cost.

Due to its characteristics, the adjoint method can be used with other algorithms that are based on the gradient of the objective function such as the Broyden–Fletcher–Goldfarb–Shanno (BFGS) method, the ellipsoidal method, among others.

The proposed optimization problem is based on the minimization of the square of the sum of electric charge of each conductor of the system given by (11) respecting the constraints of geometry and SIL which were given in Sections IV and V, respectively. So, once the SIL is a constraint in the problem, it is expected that for more complex cases (a great number of conductors) the constraints would be more difficult to be respected and this increase in the number of variables means more time of execution for CFD method. On the other hand, the sensitivity analysis using the adjoint methods is not affected by the choice of perturbation parameters and does not demand additional computational time with a bigger number of variables. We hope to do an experiment with a great number of conductors very soon to confirm this hypothesis.

Acknowledgments

This work was partially supported by CAPES, CNPq, FAPEMIG, UFMG and CEFET-MG.

References

[1] F. Kiessling, P. Nefzger, J. F. Nolasco, and U. Kaintzyk, *Overhead power lines: planning, design, construction*. Springer, 2014.

[2] A. L. Paganotti, M. M. Afonso, M. A. O. Schroeder, R. S. Alipio, E. N. Gonçalves, and R. R. Saldanha, "An adaptive deep-cut ellipsoidal algorithm applied to the optimization of transmission lines," *IEEE Transactions on Magnetics*, vol. 51, no. 3, pp. 1–4, 2015.

[3] J. S. Acosta and M. C. Tavares, "Methodology for optimizing the capacity and costs of overhead transmission lines by modifying their bundle geometry," *Electric Power Systems Research*, vol. 163, pp. 668 – 677, 2018, advances in HV Transmission Systems. [Online]. Available: http://www.sciencedirect.com/science/article/pii/S0378779617304091

[4] C. K. Arruda, L. A. M. C. Domingues, A. L. Esteves dos Reis, F. M. Absi Salas, and J. C. Salari, "The optimization of transmission lines in brazil: Proven experience and recent developments in research and development," *IEEE Power and Energy Magazine*, vol. 18, no. 2, pp. 31–42, 2020.

[5] A. EPRI, *Transmission Line Reference Book–200 kV and Above*. Electric Power Research Institute, 2005.

[6] J. F. Hall and A. K. Deb, "Prediction of overhead transmission line ampacity by stochastic and deterministic models," *IEEE Transactions on Power Delivery*, vol. 3, no. 2, pp. 789–800, 1988.

[7] A. Salari, J.C.; Reis and L. Estrella Jr, "Metodologia sistematizada para a otimização técnico-econômica da geometria dos feixes de condutores de linhas de transmissão aéreas," in *XVIII ERIAC*, 2019.

[8] S. Gomes Jr, C. Portela, and C. Fernandes, "Principles and advantages of utilizing high natural power lines and presentation of comparative results (in portuguese)-xiii snptee national seminar of production and transmission of electric energy, 6 p," *Florianópolis, Brazil*, 1995.

[9] G. N. Alexandrov, "Theory of bundle conductors," *IEEE Transactions on Power Apparatus and Systems*, vol. PAS-88, no. 6, pp. 932–936, 1969.

[10] J. S. Acosta and M. C. Tavares, "Enhancement of overhead transmission line capacity through evolutionary computing," in *2018 IEEE PES Transmission Distribution Conference and Exhibition - Latin America (T D-LA)*, pp. 1–5, 2018.

[11] M. Ghassemi, "High surge impedance loading (hsil) lines: A review identifying opportunities, challenges, and future research needs," *IEEE Transactions on Power Delivery*, vol. 34, no. 5, pp. 1909–1924, 2019.

[12] O. Regis, "Increasing the transmission capacity of overhead lines-high surge impedance loading technique," *Electra*, no. 221, 2005.

[13] M. O. B. C. Melo, L. C. A. Fonseca, E. Fontana, and S. R. Naidu, "Electric and magnetic fields of compact transmission lines," *IEEE Transactions on Power Delivery*, vol. 14, no. 1, pp. 200–204, 1999.

[14] M. O. Comber and L. E. Zaffanella, "Audible-noise reduction by bundle geometry optimization," *IEEE Transactions on Power Apparatus and Systems*, vol. PAS-92, no. 5, pp. 1782–1791, 1973.

[15] J. C. S. Filho, "Otimização da geometria dos feixes de condutores de linhas de transmissão," Master's thesis, COPPE - Universidade Federal do Rio de Janeiro, Rio de Janeiro, Abril 1993.

[16] J. S. Acosta and M. C. Tavares, "Multi-objective optimization of overhead transmission lines including the phase sequence optimization," *International Journal of Electrical Power Energy Systems*, vol. 115, p. 105495, 2020. [Online]. Available: http://www.sciencedirect.com/science/article/pii/S0142061519303382

[17] R. de Paula Maciel, "Maximização da potência característica de linhas de transmissão usando método de otimização não linear," Master's thesis, Universidade Estadual de Campinas, Faculdade de Engenharia Elétrica e Computação, Campinas, Março 2013.

[18] I. A. M. Duane, M. M. Afonso, M. A. de Oliveira Schroeder, S. T. M. Gonçalves, A. L. Paganotti, and R. R. Saldanha, "A new strategy for optimizing hsil transmission lines," *Journal of Control, Automation and Electrical Systems*, vol. 31, no. 5, pp. 1288–1297, 2020.

[19] R. R. Saldanha, R. H. C. Takahashi, J. A. Vasconcelos, and J. A. Ramirez, "Adaptive deep-cut method in ellipsoidal optimization for electromagnetic design," *IEEE Transactions on Magnetics*, vol. 35, no. 3, pp. 1746–1749, 1999.

[20] M. Bakr, A. Z. Elsherbeni, and V. Demir, *Adjoint sensitivity analysis of high frequency structures with Matlab*. The Institution of Engineering and Technology, 2017.

[21] M. Bakr, *Nonlinear optimization in electrical engineering with applications in matlab*. Institution of Engineering and Technology, 2013.

[22] M. S. Dadash, N. K. Nikolova, and J. W. Bandler, "Analytical adjoint sensitivity formula for the scattering parameters of metallic structures," *IEEE Transactions on Microwave Theory and Techniques*, vol. 60, no. 9, pp. 2713–2722, 2012.

[23] N. K. Nikolova, J. W. Bandler, and M. H. Bakr, "Adjoint techniques for sensitivity analysis in high-frequency structure cad," *IEEE Transactions on Microwave Theory and Techniques*, vol. 52, no. 1, pp. 403–419, 2004.

[24] D. G. Luenberger, Y. Ye, *et al.*, *Linear and nonlinear programming*. Springer, 1984, vol. 2.

[25] S. Director and R. Rohrer, "The generalized adjoint network and network sensitivities," *IEEE Transactions on Circuit Theory*, vol. 16, no. 3, pp. 318–323, 1969.

[26] C. A. Balanis, *Advanced engineering electromagnetics*. John Wiley & Sons, 1998.

Brazilian Microwave and Optoelectronics Society-SBMO received 29 Jan 2021; for review 29 Jan 2021; accepted 29 Apr 2021
Brazilian Society of Electromagnetism-SBMag *ISSN 2179-1074*

[27] J. D. Glover, M. S. Sarma, and T. Overbye, *Power system analysis & design, SI version*. Cengage Learning, 2012.
[28] M. P. Sarma and W. Janischewskyj, "Electrostatic field of a system of parallel cylindrical conductors," *IEEE Transactions on Power Apparatus and Systems*, vol. PAS-88, no. 7, pp. 1069–1079, 1969.
[29] C. J. Miller, "The calculation of radio and corona characteristics of transmission-line conductors," *Transactions of the American Institute of Electrical Engineers. Part III: Power Apparatus and Systems*, vol. 76, no. 3, pp. 461–472, 1957.
[30] H. Lee and N. Ida, "An interpretation of adjoint sensitivity analysis for shape optimal design of electromagnetic systems," in *9th IET International Conference on Computation in Electromagnetics (CEM 2014)*, pp. 1–2, 2014.
[31] N. K. Georgieva, S. Glavic, M. H. Bakr, and J. W. Bandler, "Feasible adjoint sensitivity technique for em design optimization," *IEEE Transactions on Microwave Theory and Techniques*, vol. 50, no. 12, pp. 2751–2758, 2002.
[32] ANEEL, *Resolução Normativa nº 616, de 1 de julho de 2014 (in portuguese)*, Agência Nacional de Energia Elétrica, Brasília, DF, 1 jul. 2014.
[33] ABNT, *NBR 25415: Métodos de medição e níveis de referência para exposição a campos elétricos e magnéticos na frequência de 50 Hz e 60 Hz (in portuguese)*, Associação Brasileira de Normas Técnicas, Rio de Janeiro, jul. 2016.
[34] ICNIRP, *Guidelines for Limiting Exposure to Time-varying Electric and Magnetic Fields (1 Hz to 100 kHz)*, International Commission on Non-Ionizing Radiation Protection, 2010.
[35] O. Régis Jr, F. C. DART, A. L. P. CRUZ, and C. C. CHESF, "Avaliação comparativa das concepções de linhas de potência natural elevada em 500 kv utilizadas no brasil," *XIII ERIAC*, 2009.

Brazilian Microwave and Optoelectronics Society-SBMO *received 29 Jan 2021; for review 29 Jan 2021; accepted 29 Apr 2021*
Brazilian Society of Electromagnetism-SBMag *ISSN 2179-1074*